Flow of a circulating tumor cell and red blood cells in microvessels

Naoki Takeishi,[1] Yohsuke Imai,[2,*] Takami Yamaguchi,[1] and Takuji Ishikawa[2]
[1]*Graduate School of Biomedical Engineering, Tohoku University, 6-6-01 Aoba, Aoba, Sendai 980-8579, Japan*
[2]*School of Engineering, Tohoku University, 6-6-01 Aoba, Aoba, Sendai 980-8579, Japan*
(Received 27 April 2015; published 9 December 2015)

Quantifying the behavior of circulating tumor cells (CTCs) in the blood stream is of fundamental importance for understanding metastasis. Here, we investigate the flow mode and velocity of CTCs interacting with red blood cells (RBCs) in various sized microvessels. The flow of leukocytes in microvessels has been described previously; a leukocyte forms a train with RBCs in small microvessels and exhibits margination in large microvessels. Important differences in the physical properties of leukocytes and CTCs result from size. The dimensions of leukocytes are similar to those of RBCs, but CTCs are significantly larger. We investigate numerically the size effects on the flow mode and the cell velocity, and we identify similarities and differences between leukocytes and CTCs. We find that a transition from train formation to margination occurs when $(R-a)/t^R \approx 1$, where R is the vessel radius, a is the cell radius, and t^R is the thickness of RBCs, but that the motion of RBCs differs from the case of leukocytes. Our results also show that the velocities of CTCs and leukocytes are larger than the average blood velocity, but only CTCs move faster than RBCs for microvessels of $R/a \approx 1.5$–2.0. These findings are expected to be useful not only for understanding metastasis, but also for developing microfluidic devices.

DOI: 10.1103/PhysRevE.92.063011 PACS number(s): 47.63.Jd, 47.57.E−, 87.19.xj, 87.85.gf

I. INTRODUCTION

A total of 90% of cancer-related deaths result from metastasis, whereby tumor cells are shed from a primary tumor and circulate with the flow of blood. Such circulating tumor cells (CTCs) adhere to the blood vessels in distant organs, where they form secondary tumors [1–3]. The metastatic process involves both the solid and fluid mechanics of blood cells, but how CTCs flow with red blood cells (RBCs) in the blood stream remains unclear [4]. The behavior of CTCs is also of fundamental importance in the design of microfluidic devices. Although the number of CTCs in peripheral blood is very small, the concentration of CTCs should be precisely characterized to diagnose the progress of cancer and to evaluate the efficacy of anticancer drugs. For this purpose, microfluidic devices are currently under development, with the aim of separating CTCs from blood samples [5,6]. Hence, understanding the flow modes of CTCs and RBCs in microvessels, including the cell velocities, is helpful in the design of novel microfluidic devices.

Here, we investigate the flow of a single CTC and RBCs in microvessels of various diameters. The flow mode of a leukocyte and RBCs has been well described in previous studies [7–12]. A leukocyte forms a train with RBCs in small microvessels. As the vessel size increases, the RBCs exhibit axial migration, whereas the leukocytes flow near the wall in a process termed "margination." Because of the inner structure consisting of actin filaments, microtubules, and intermediate filaments, the deformability of leukocytes is much less than that of RBCs. It has been reported that the stiffness of leukocytes is a dominant factor for margination [10,13]. CTCs have an inner structure similar to that of leukocytes, and their behavior is expected to be similar to that of leukocytes. Although the size of leukocytes varies, the most abundant type, neutrophils, are approximately 4 μm in radius, similar to RBCs. CTCs are typically a few times larger than leukocytes [14,15], and hence the primary objective of this study is to investigate the similarities and differences between the flow modes of leukocytes and RBCs. The second objective is to quantify the velocity of CTCs in microvessels, i.e., do they move downstream faster or slower than the mean volume of blood? In general, a particle located at the center of a channel moves faster than the average velocity of the suspension because of the parabolic velocity profile. Therefore, the velocity of the CTC may be higher compared to the average blood velocity when it forms a train, but the CTC velocity may be lower if the cell is marginated.

We carried out numerical simulations of the flow of a CTC and RBCs in microvessels, whereby the CTC was modeled as a large spherical capsule, and the RBCs were modeled as small biconcave capsules. We found that the flow mode of the CTC with RBCs underwent a transition from train formation to margination as the diameter of the vessel increased. Because of the size differences between CTCs and RBCs, the motion of RBCs differed from the case of leukocytes. We also found that both leukocytes and CTCs flowed faster than the mean blood velocity, but only CTCs were faster than RBCs.

II. METHODS

A. Flow and cell models

Consider a cellular flow consisting of plasma, RBCs, and a CTC in a microvessel. The microvessel was modeled as a cylindrical channel of radius R. The length of the computational domain was approximately 100 μm, and periodic boundary conditions were employed. The plasma was assumed to be a Newtonian fluid with a viscosity of $\mu^P = 1.2 \times 10^{-3}$ Pa s. The RBCs were modeled as biconcave capsules with a radius of $a^R = 4$ μm and a thickness of $t^R = 2$ μm, filled with a Newtonian fluid of viscosity $\mu^R = 6 \times 10^{-3}$ Pa s, and enclosed by a hyperelastic membrane. The membrane was assumed to follow the constitutive law proposed by Skalak

*yimai@pfsl.mech.tohoku.ac.jp

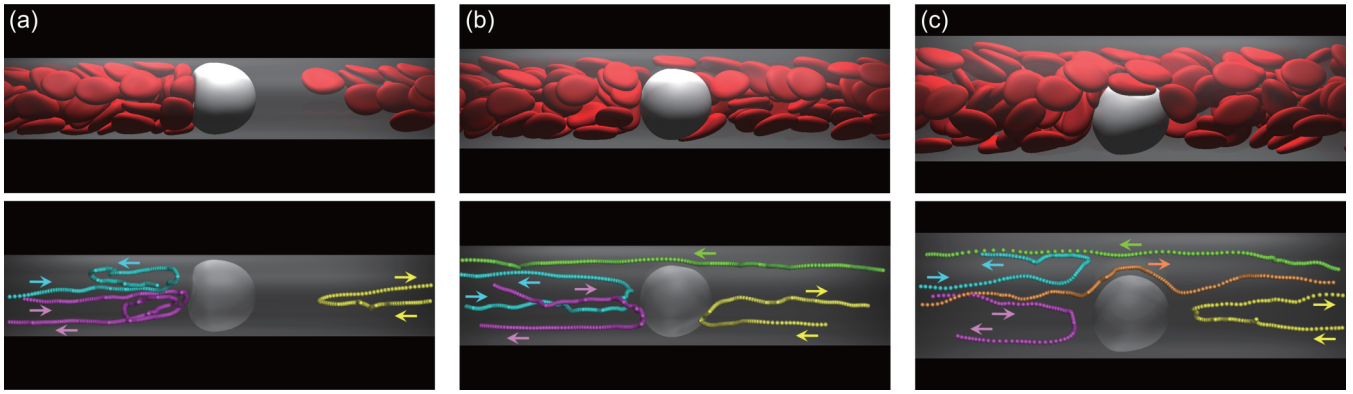

FIG. 1. (Color online) Flow modes of a CTC ($a = 8\ \mu$m) with RBCs ($a^R = 4\ \mu$m, $t^R = 2\ \mu$m) in microvessels. Flow direction is from left to right. Trajectories of sample RBCs are also shown. (a) Train formation for $R = 9\ \mu$m [$(R-a)/t^R = 0.5$], where the RBCs behind the CTC exhibit a recirculating motion. (b) Margination for $R = 11\ \mu$m [$(R-a)/t^R = 1$], where the CTC overtakes the RBCs. (c) Margination for $R = 13\ \mu$m [$(R-a)/t^R = 1.5$], where the CTC is overtaken by some RBCs. The hematocrit value was 0.2 for all cases. See also the Supplemental Material [16].

et al. [17], i.e.,

$$w = \frac{G}{2}\left(I_1^2 + 2I_1 - 2I_2 + CI_2^2\right), \tag{1}$$

where w is the strain energy density function, G is the surface shear elastic modulus, C is the coefficient of the area dilation modulus, and I_1 and I_2 are the invariants of the strain tensor. The surface shear elastic modulus is given by $G^R = 4\ \mu$N/m [12], mimicking the stretching of RBCs by optical tweezers [18]. The area dilation modulus was $C^R = 10^2$, which describes the almost incompressible membrane of the RBCs. The bending resistance was also considered [19], with a bending modulus of $k_b^R = 5.8 \times 10^{-19}$ N m [20].

The CTC was modeled as a spherical capsule with a radius of $a = 8\ \mu$m [14,15]. CTCs have a cytoskeleton consisting of actin filaments, microtubules, and intermediate filaments, which makes them less deformable than RBCs [21]. Therefore, the CTC was modeled as a stiffer capsule than the RBCs, with $R_G = G/G_R = 10^2$. The other parameters remained the same (i.e., $C = C^R$, $\mu = \mu^R$, and $k_b = k_b^R$). The problem was characterized by the capillary number $\mathrm{Ca} = \mu\dot{\gamma}a^R/G^R$, where $\dot{\gamma} = U_m/2R$ is the mean shear rate and U_m is the mean velocity. A fixed capillary number of $\mathrm{Ca} = 0.2$ was used to mimic microcirculation. Ligand-receptor interactions between CTCs and endothelial cells were neglected, as the focus was on hydrodynamic processes.

B. Numerical method

The finite-element method (FEM) was used to describe the membrane mechanics [22], so that we have

$$\int_S \hat{\boldsymbol{u}} \cdot \boldsymbol{q}\, dS = \int_S \hat{\boldsymbol{\varepsilon}} : \boldsymbol{T}\, dS, \tag{2}$$

where $\boldsymbol{T}$ is the Cauchy stress tensor, $\boldsymbol{q}$ is the load on the membrane, $\hat{\boldsymbol{u}}$ is the virtual displacement, and $\hat{\boldsymbol{\varepsilon}}$ is the virtual strain. The lattice-Boltzmann method (LBM) was used to describe the fluid mechanics [23], i.e.,

$$f_i(\boldsymbol{x} + \boldsymbol{c}_i\Delta t, t + \Delta t) - f_i(\boldsymbol{x}, t) = -\frac{1}{\tau}\left[f_i(\boldsymbol{x}, t) - f_i^{\mathrm{eq}}(\boldsymbol{x}, t)\right] + F_i\Delta t, \tag{3}$$

where f_i is the particle distribution function for particles with velocity $\boldsymbol{c}_i$ at the position $\boldsymbol{x}$, Δt is the time step size, f_i^{eq} is the equilibrium distribution function, τ is the nondimensional relaxation time, and F_i is the external force term. The D3Q19 lattice model was used.

The FEM model for membrane mechanics was coupled with the LBM for fluid mechanics using an immersed boundary method [24]. The volume-of-fluid method [25] and front-tracking method [26] were also employed to update the viscosity in the fluid mesh. All procedures were implemented on a graphics processing unit (GPU) [27]. Our method was validated using test problems including the deformation of RBCs in shear flow and the thickness of cell-depleted

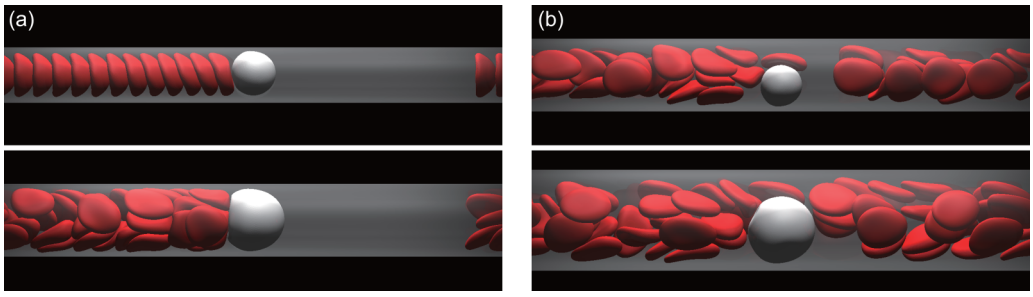

FIG. 2. (Color online) (a) (top) Train formation of a leukocyte ($a = 4\ \mu$m) and (bottom) train formation of a small CTC ($a = 6\ \mu$m) with RBCs in microvessels. (b) (top) Margination of a leukocyte and (bottom) margination of a small CTC.

peripheral layers in channel flows; the model was also applied successfully to simulate leukocyte margination [12]. The mesh size of the LBM was 0.25 μm, and that of the FEM model was also approximately 0.25 μm. The mesh sizes were the same as those used in [12].

III. RESULTS

A. Train formation and margination

Figure 1 shows snapshots of typical numerical results, with trajectories of sample RBCs with $Hct = 0.2$ (see the Supplemental Material [16]). In a small microvessel (i.e., $R = 9$ μm), the CTC flowed in the center of the vessel, followed by the RBCs, which exhibited a recirculating motion, whereby as an RBC approached the CTC in the center of the vessel, it returned to the wall. When the vessel size was increased to $R = 11$ μm, the CTC began to overtake the RBCs. This motion induced lateral migration of the CTC; this is termed margination in this paper. As the vessel size was further increased to $R = 13$ μm, some RBCs passed forward, although the CTC was faster than most RBCs. To examine the effects of cell size on flow mode, we also simulated the flow of a leukocyte ($a = 4$ μm) with RBCs, as well as that of a small CTC ($a = 6$ μm) with RBCs with various microvessel sizes. Both cell types exhibited train formation and margination, as shown in Fig. 2. However, where train formation occurred with the leukocyte, the RBCs exhibited a parachute shape deformation and simply followed the leukocyte in single file.

B. Radial location

We compared the radial locations of the leukocyte and CTCs. The radial locations normalized to the vessel radius r/R are shown in Fig. 3 for three values of Hct as a function of the normalized vessel radius R/a. The normalized radial locations of the cells increased as the vessel radius increased. When the cells marginated, the normalized positions were similar among all three cell types, although larger cells maintained their radial position near the wall more stably.

C. Cell velocity of CTCs

We examined the velocities of three cells. Bungay and Happel proposed an analytical expression for rigid spheres with $R/a \approx 1$ [28]. Figure 4 shows the numerical results together with those of this analytical expression, where the cell velocity V_C was normalized to the average blood velocity V_B. As shown in Fig. 4, $V_C/V_B > 1$ for all values of R/a and Hct. With train formation, for small R/a values, the normalized cell velocity was similar to or slightly smaller than the analytical result for all cell sizes. When the cell marginated, the cell velocity diverged from the analytical result, but it remained higher than the average blood velocity. Note that the cell velocity was slightly smaller for larger cells; this is because margination was more stable for larger cells than smaller cells.

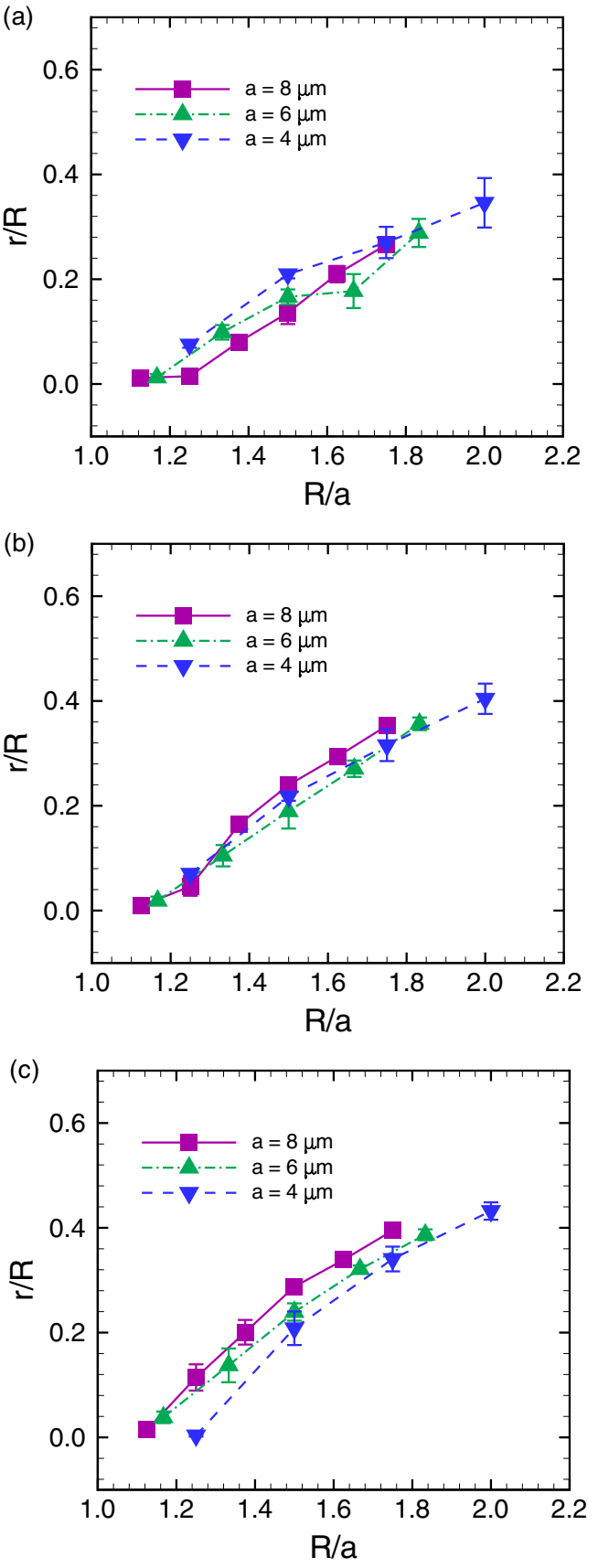

FIG. 3. (Color online) The radial location of cells in various diameter microvessels with (a) $Hct = 0.1$, (b) $Hct = 0.2$, and (c) $Hct = 0.3$.

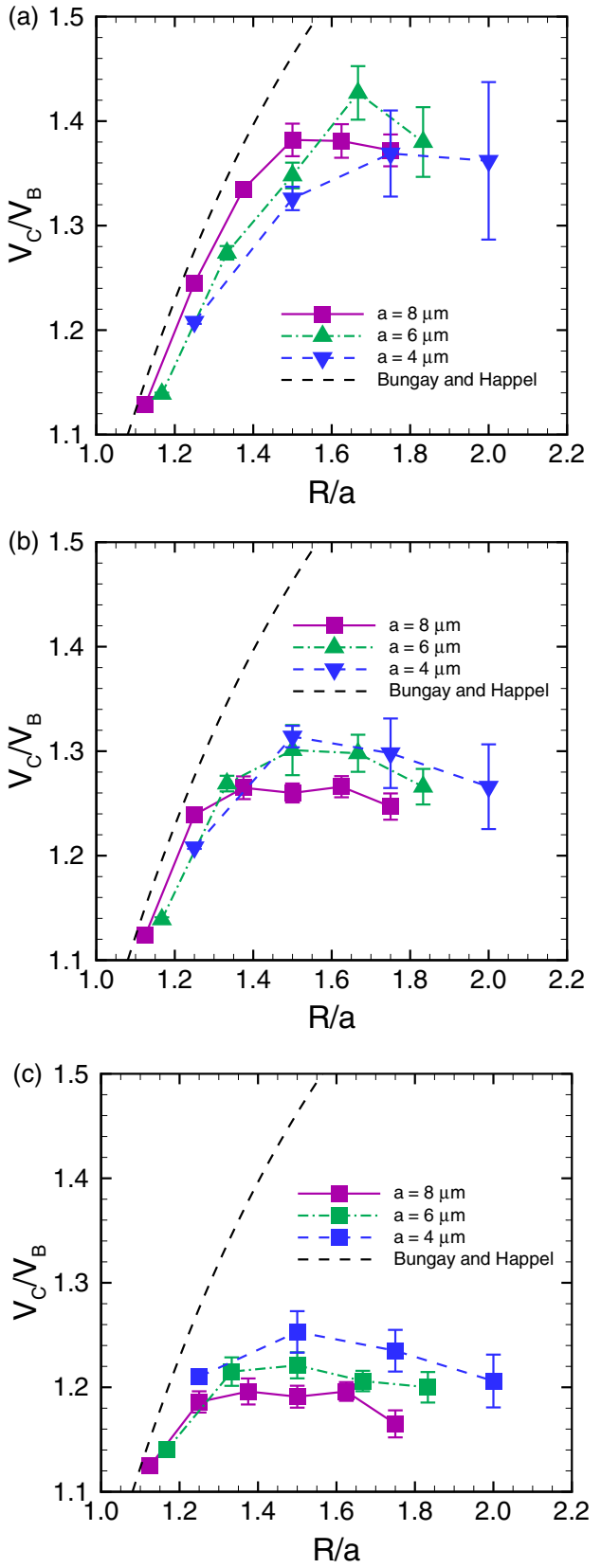

FIG. 4. (Color online) Ratio of cell velocity to the average blood velocity for various diameter microvessels. (a) $Hct = 0.1$, (b) $Hct = 0.2$, and (c) $Hct = 0.3$. Analytical solutions are also shown using the expression reported by Bungay and Happel [28], with $r/R = 0$ and $R/a \approx 1$.

IV. DISCUSSION AND CONCLUSION

A. Flow mode changes from train to margination at $(R-a)/t^R > 1$

Although it is known that CTCs are arrested within very small microvessels due to the size restriction [1,29], their behavior under the flow condition is not fully understood. Hence, the first objective of this study was to describe the behavior of CTCs in various sized microvessels.

The flow mode of CTCs in a small microvessel was similar to the train formation that occurred with a leukocyte and RBCs [7,12], although there were some differences in RBC motion. RBCs located behind the leukocyte exhibited a parachute-shaped deformation and simply followed the leukocyte in single file, whereas those behind the CTC exhibited a recirculating motion [Figs. 1(a) and 2(a)]. As the vessel size increased, the CTC exhibited margination, as did the leukocyte and the small CTC [Figs. 1(b) and 2(b)]. Even with the low deformability of the CTC, it experienced lift forces from the wall and the shear gradient, and the hydrodynamic collision forces from the RBCs were required to maintain the position near the wall. During the overtaking motions, RBCs effectively push the CTC toward the wall, resulting in margination of the CTCs via the same mechanism as with leukocyte and capsule marginations [12,30]. The stiffness of the CTC indeed plays an important role in margination. Leukocyte margination is reduced when the stiffness of leukocytes becomes softer [10], and a systematic study on the effects of particles size and stiffness on margination is found in [13]. As these previous studies suggested, margination was discouraged when the deformability of the CTC was set to be the same as RBCs.

To describe the flow modes of the leukocytes and CTCs quantitatively, we plotted a diagram showing the flow modes, which indicates the cell velocity relative to the average velocity of the RBCs. When a cell forms a train with the RBCs, the relative velocity should be almost zero. When a cell is marginated and overtakes the RBCs, the relative velocity is positive; when the cell is overtaken by RBCs, the relative velocity is negative. Figures 5(a), 5(b), and 5(c) represent diagrams of flow modes for $Hct = 0.1$, 0.2, and 0.3, respectively. The relative velocity during train formation was assumed to be negligibly small, $|V_C - V_R|/V_B < \epsilon = 0.005$, where V_C is the cell velocity, V_R is the average velocity of RBCs, and V_B is the average velocity of the blood. With $Hct = 0.2$ (a physiologically relevant hematocrit for microcirculation), both the leukocyte and CTCs exhibited train formation with RBCs when the gap between the cell and the wall was smaller than the thickness of the RBCs, $(R-a)/t^R < 1$. When the gap became larger than the thickness of the RBCs [$(R-a)/t^R > 1$], a transition from train formation to margination occurred, both for the leukocyte and CTCs, whereby the CTC overtook the RBCs and the leukocyte was overtaken by the RBCs. The small CTC first overtook the RBCs and was then overtaken by the RBCs over the range of vessel sizes investigated. With $Hct = 0.3$, a transition from train formation to margination occurred for $(R-a)/t^R \approx 1$ or larger; however, low hematocrit cases appear to be exceptional, and the flow mode of CTCs remained as train formation even for $(R-a)/t^R = 2$ at $Hct = 0.1$.

The normalized radial positions were comparable for marginated cells when plotted as a function of the normalized

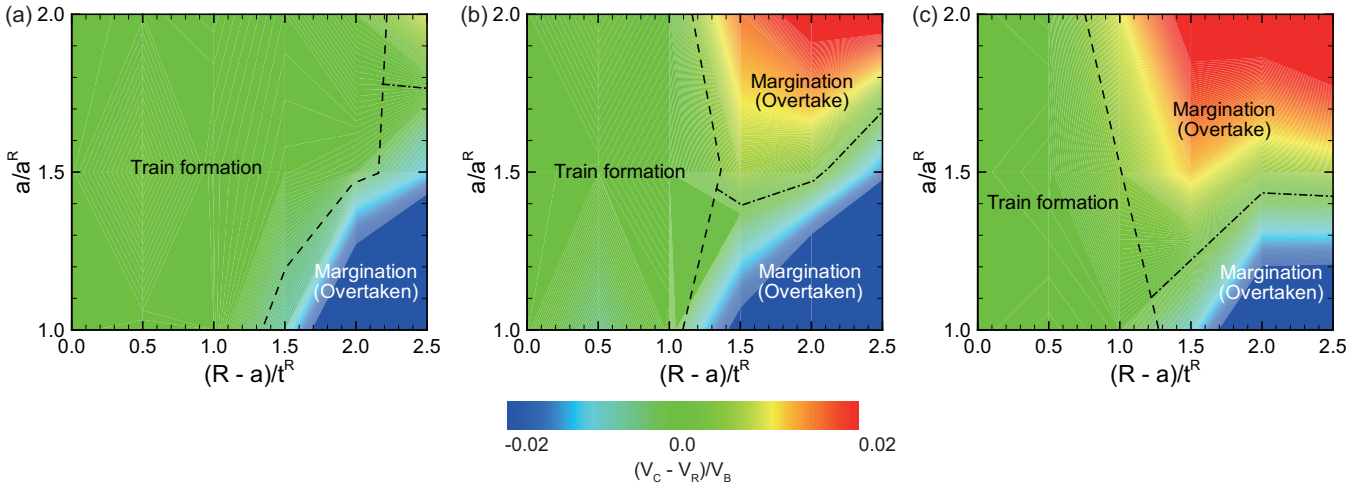

FIG. 5. (Color online) Comparison of flow modes. The flow modes as functions of $(R-a)/t^R$ and a/a^R for (a) $Hct = 0.1$, (b) $Hct = 0.2$, and (c) $Hct = 0.3$. Here, the color contours represent the cell velocity relative to the average velocity of the RBCs [i.e., $(V_C - V_R)/V_B$], the dashed lines show $|V_C - V_R|/V_B < \epsilon = 0.005$, and the dash-dot lines show $(V_C - V_R)/V_B = 0$.

vessel radius R/a. These results suggest that when leukocytes and CTCs are present in the same blood flow, their radial locations will differ because of the different values of R/a. Moreover, designing a microfluidic device should be possible so that leukocytes are marginated and CTCs form trains.

B. CTCs move faster than the mean blood velocity

An important question is whether the CTCs move downstream faster or slower than the mean blood velocity. The hematocrit of RBCs at the outlet of a microvessel (i.e., the discharge hematocrit) increased compared with that at the inlet (i.e., the tube hematocrit). This is referred to as the Fåhræus effect [31], and it is a consequence of axial migration of RBCs and the parabolic velocity profile of channel flow. The same mechanism may lead to a larger velocity of the CTC compared to the average blood velocity when it forms a train with the RBCs, but the CTC velocity may be lower if the cell is marginated.

The velocities of the leukocyte and CTCs were larger than the average blood velocity when they formed trains, as expected (Fig. 4). The normalized cell velocity V_C/V_B followed closely, or was slightly lower than that predicted by the analytical expression for a rigid sphere [28].

As shown in Fig. 4, we found that V_C/V_B was greater than unity for the entire range of R/a and Hct examined in this study. This result suggests that leukocytes and CTCs flow faster than the average blood velocity, even when marginated. Note that if the vessel diameter increases further, the values are expected to decrease, so that we have $V_C/V_B \to 0$ as $R/a \to \infty$. Hence, a larger cell velocity than the average blood velocity is expected, at least when the radius of the microvessel is a few times larger than the cell radius. Such a larger velocity than the average blood velocity was also reported for a leukocyte in a microvessel, where $R/a = 2$ [11]. These results suggest that leukocytes and CTCs can be efficiently enriched at the outlet of a microfluidic device when $R/a \approx 1.5$–2.0. In addition, as shown in Fig. 5, the CTC flowed faster than the RBCs; in contrast, the velocity of a leukocyte ($a = 4\ \mu$m) was always smaller than the average RBC velocity.

In conclusion, we found that the flow mode of a CTC with RBCs in microvessels was similar to that of a leukocyte with RBCs. A transition from train formation to margination occurred at $(R-a)/t^R \approx 1$. The ratio of the CTC velocity (or the leukocyte velocity) to the average blood velocity in the train formation is well described by the analytical result of Bungay and Happel [28]. The cell velocities of CTCs and leukocytes were larger than the average blood velocity, even when marginated. Moreover, only CTCs moved faster than RBCs, and they can be enriched efficiently at the outlet of microchannels with $R/a \approx 1.5$–2.0.

ACKNOWLEDGMENTS

This research was supported by JSPS KAKENHI Grant Nos. 24680048, 25000008, 26107703, and 14J03967. We also acknowledge support from the Tohoku University Division for International Advanced Research and Education Organization.

[1] A. F. Chambers, A. C. Groom, and I. C. MacDonald, Nat. Rev. Cancer **2**, 563 (2002).
[2] G. P. Gupta and J. Massague, Cell **127**, 679 (2006).
[3] D. Wirtz, K. Konstantopoulos, and P. C. Searson, Nat. Rev. Cancer **11**, 512 (2011).
[4] P. Koumoutsakos, I. Pivkin, and F. Milde, Annu. Rev. Fluid Mech. **45**, 325 (2013).
[5] C. T. Lim and D. S. B. Hoon, Phys. Today **67**(2), 26 (2014).
[6] T. Tanaka, T. Ishikawa, K. Numayama-Tsuruta, Y. Imai, H. Ueno, N. Matsuki, and T. Yamaguchi, Lab Chip **12**, 4336 (2012).
[7] G. W. Schmid-Shönbein, S. Usami, R. Skalak, and S. Chien, Microvasc. Res. **19**, 45 (1980).
[8] H. L. Goldsmith and S. Spain, Microvasc. Res. **27**, 204 (1984).
[9] J. B. Freund, Phys. Fluids **19**, 023301 (2007).

[10] D. A. Fedosov, J. Fornleitner, and G. Gompper, Phys. Rev. Lett. **108**, 028104 (2012).
[11] D. A. Fedosov and G. Gompper, Soft Matter **10**, 2961 (2014).
[12] N. Takeishi, Y. Imai, K. Nakaaki, T. Yamaguchi, and T. Ishikawa, Physiol. Rep. **2**, e12037 (2014).
[13] A. Kumar, R. G. H. Rivera, and M. D. Graham, J. Fluid Mech. **738**, 423 (2014).
[14] S. L. Stott, C.-H. Hsu, D. I. Tsukrov, M. Yu, D. T. Miyamoto, B. A. Waltman, S. M. Rothenberg, A. M. Shah, M. E. Smas, G. K. Korir, F. P. Floyd Jr., A. J. Gilman, J. B. Lord, D. Winokur, S. Springer, D. Irimia, S. Nagrath, L. V. Sequist, R. J. Lee, K. J. Isselbacher, S. Maheswaran, D. A. Haber, and M. Toner, Proc. Natl. Acad. Sci. (USA) **107**, 18392 (2010).
[15] R. A. Harouaka, M. Nisic, and S.-Y. Zheng, J. Lab. Automat. **18**, 455 (2013).
[16] See Supplemental Material at http://link.aps.org/supplemental/10.1103/PhysRevE.92.063011 for movies showing the flow mode of a CTC with RBCs.
[17] R. Skalak, A. Tozeren, P. R. Zarda, and S. Chien, Biophys. J. **13**, 245 (1973).
[18] S. Suresh, J. Spatz, J. P. Micoulet, M. Dao, C. T. Lim, M. Beil, and T. Seufferlein, Acta Biomater. **1**, 15 (2005).
[19] J. Li, M. Dao, C. T. Lim, and S. Suresh, Biophys. J. **88**, 3707 (2005).
[20] M. P. de Morales–Marinkovic, K. T. Turner, J. P. Butler, J. J. Fredberg, and S. Suresh, Am. J. Physiol. Cell Physiol. **293**, C597 (2007).
[21] M. Li, L. Q. Liu, N. Xi, Y. C. Wang, Z. L. Dong, X. B. Xiao, and W. J. Zhang, Sci. China Life Sci. **55**, 968 (2012).
[22] J. Walter, A.-V. Salsac, D. Barthès-Biesel, and P. Le Tallec, Int. J. Numer. Meth. Eng. **83**, 829 (2010).
[23] S. Chen and G. D. Doolen, Annu. Rev. Fluid Mech. **30**, 329 (1998).
[24] C. S. Peskin, Acta Numer. **11**, 479 (2002).
[25] K. Yokoi, J. Comput. Phys. **226**, 1985 (2007).
[26] S. O. Unverdi and G. Tryggvason, J. Comput. Phys. **100**, 25 (1992).
[27] T. Miki, X. Wang, T. Aoki, Y. Imai, T. Ishikawa, K. Takase, and T. Yamaguchi, Comput. Meth. Biomech. Biomed. Eng. **15**, 771 (2012).
[28] P. M. Bungay and H. Brenner, Int. J. Multiphase Flow **1**, 25 (1973).
[29] A. F. Chambers, I. C. MacDonald, E. E. Schmid, S. Koop, V. L. Morris, R. Khokha, and A. C. Groom, Cancer Metast. Rev. **14**, 279 (1995).
[30] A. Kumar and M. D. Graham, Soft Matter **8**, 10536 (2012).
[31] A. R. Pries, D. Neuhaus, and P. Gaehtgens, Am. J. Physiol. **263**, H1770 (1992).